Genes Determining Nevus Count and Dermoscopic Appearance in Australian Melanoma Cases and Controls

Journal of Investigative Dermatology (2020) **140,** 498–501; doi:10.1016/j.jid.2019.05.032

TO THE EDITOR

Total body nevus counts (TNC) is a highly heritable trait, with twin studies estimating that 60% to 70% of its variance is explained by genetic factors (Lee et al., 2016). Polymorphisms within *IRF4, MTAP, PLA2G6,* and *MITF* have been shown to strongly influence TNC, and many other nevus-associated genes have been recognized (Duffy et al., 2018). Dermoscopy has allowed the recognition of distinct morphological classes of nevi, including reticular, globular, and homogenous and/or complex, that tightly correlate with histopathological subtypes (Tan et al., 2019). There has been great interest in the clinical presentation (Suh and Bolognia, 2009), body site density (Bataille et al., 1996; Blake et al., 2014), dermoscopic growth pattern, and anatomical distribution of nevi (Bajaj et al., 2015; Fonseca et al., 2015; Marchetti et al., 2014) in relation to the cutaneous melanoma (CM) risk (Ribero et al., 2016). In this study, we test the association between the number of nevi of each morphology and melanoma risk and whether known nevus loci predispose to particular nevus morphologies in a genome-wide association study of melanoma cases and controls within the Brisbane Nevus Morphology Study (BNMS).

We captured dermoscopic images for 27,221 nevi $\geq$ 5mm in diameter from 1,266 individuals, classified by subtype using two methods (McWhirter et al., 2017), which were pooled for analysis (see Supplementary Materials). In the combined dataset, the dominant nevus subtype pattern was nonspecific (homogenous 46% and/or complex 37%), followed by reticular (11%), and then globular pattern (5%). On average, the number of nevi in each subtype was higher in the cases than the controls, with nonspecific at 24.2 versus 9.3, reticular at 5.2 versus 2.2, and globular at 2.7 versus 1.8 (Supplementary Table S1).

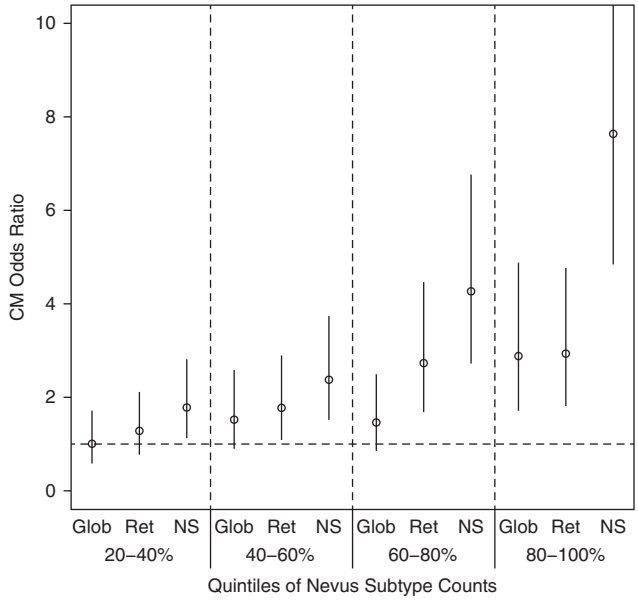

Figure 1. Odds ratio for cutaneous melanoma by nevus subtypes. CM odds ratio and 95% CI (x-axis) is plotted by quintile (y-axis) of the three nevus subtypes: globular, reticular, and nonspecific. The first quintile set to 1 (0-20%) is not shown. CI, confidence interval; CM, cutaneous malignanat melanoma; Glob, globular; NS, nonspecific; Ret, reticular

The odds ratio (OR) for CM on the quintiles of the nevus subtype counts, compared with the lowest quintile (0% to 20% set to 1) for each subtype are shown in Figure 1 (Supplementary Table S2). There was a significant increase in each of the four quintile comparisons of nonspecific subtype count, the greatest being in the highest quintile of counts for each subtype, with an OR of 7.64 (95% confidence interval [CI] = 4.86-12.19) for nonspecific nevi. In the subsample where complex and homogenous counts were available, the homogenous count was the most strongly associated phenotype for CM with OR of 11.34 (95% CI = 5.63-23.75) for the top quintile of homogenous nevi; for complex nevi, OR of 4.75 (95% CI = 2.40-9.62) (Supplementary Tables S3 and S4). Despite the reduction of globular subtype counts with age, the OR was 2.82 (95% CI = 1.72-4.88), with reticular subtype count OR of 2.94 (95% CI = 1.84-4.77), also a significant predictor of risk (Supplementary Table S2).

The genome-wide association analysis of melanoma, TNC, and nevus subtypes was performed on 1,235 BNMS participants with single nucleotide polymorphism (SNP) genotype and phenotype data available. Figure 2 shows Manhattan plots of the *P*-values

Abbreviations: BNMS, Brisbane Nevus Morphology Study; CI, confidence interval; CM, cutaneous melanoma; OR, Odds Ratio; SNP, single nucleotide polymorphism; TNC, total nevus count

Accepted manuscript published online 15 August 2019; corrected proof published online 4 December 2019

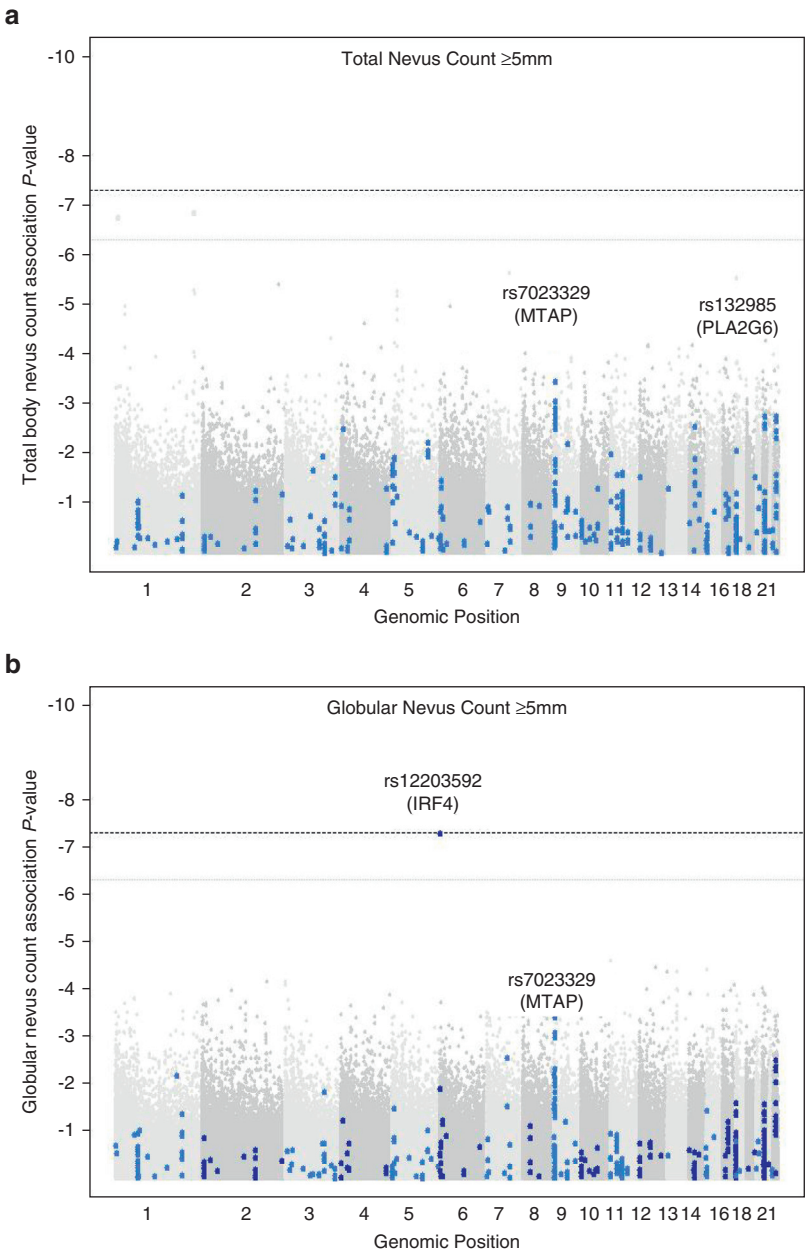

Figure 2. Genome-wide association study plot for total nevus count and globular nevus count. Manhattan plot of *P*-values for (**a**) TNC ≥ 5mm and (**b**) globular nevus count ≥ 5mm with genome-wide significance indicated by the black dashed line ($5x10^{-8}$) and suggestive of significance ($5x10^{-7}$) by the gray dotted line. Blue dots indicate the SNPs within previously associatied peaks, and the gray dots represent all other SNPs on the Illumina HumanCoreExome array. The peak-associated SNP rs7023329 on chromosome 9 is indicated as *MTAP*, rs132985 on chromosome 22 as *PLA2G6*, and rs12203592 on chromosome 6 as *IRF4*. SNP, single nucleotide polymorphism.

for the SNPs across the genome (gray) for (i) TNC and (ii) globular nevus counts, overlaid with the SNPs of significance in each peak for 32 melanoma or nevus loci (blue) from our recent genome-wide association study meta-analyses of melanoma and TNC (Duffy et al., 2018; Law et al., 2015). The SNPs of greatest significance for the TNC in these candidates (Supplementary Table S5) are within the *MTAP* ($P = 2x10^{-6}$) and *PLA2G6* ($P = -1.7x10^{-3}$) loci, with the *SLC45A2* rs250417 SNP ($P = 2x10^{-5}$) being protective, but do not in themselves reach genome-wide significance, as expected given the sample size. One SNP in the *IRF4* gene rs12203592*C/T ($P = 7x10^{-8}$) reached a level close to genome-wide significance when globular nevi were considered alone but not for the total nevus count (Figure 2b, Supplementary Table S5). Notably, this polymorphism was first reported to influence TNC in an age-dependent manner (Duffy et al., 2010), with its genotypic-specific effect on globular nevus counts consistent with the loss of globular nevi with age (Supplementary Figure S1). The SNPs within the *MTAP* locus were also consistently associated with globular nevus count, but none achieved $P < 10^{-4}$. For reticular and nonspecific nevus counts (Supplementary Figure S2), the SNPs within the *MTAP* locus are again the highest of the candidate genes, with the most significant SNP rs7036656 ($P = 2.5x10^{-5}$) located near the flanking *CDKN2A* gene.

In the case of melanoma, the most strongly associated candidate genes in the BNMS, compared with a larger number of controls drawn from the QIMR Brisbane Longitudinal Twin Study and other studies (Duffy et al., 2018), were *MTAP*, *PLA2G6*, *IRF4*, *FMN1*, *MC1R*, *ASIP*, and *SLC45A2*. There were 26 BNMS individuals who were carriers of the *MITF* E319K variant rs149617956*G/A, which as expected was highly associated with both melanoma and TNC (Supplementary Table S5).

The goals of the BNMS were to assess the natural history of the dermoscopic morphological subtypes of nevi, examine the relationship of subtype counts to CM, and identify genetic risk factors for CM for which these counts would be the intermediate step in pathogenesis. We found that the number of homogenous subtype nevi was the most highly associated with CM risk, followed by the complex pattern, then reticular and globular. This is consistent with the transition of other dermoscopic patterns to a nonspecific morphology with increasing age (Zalaudek et al., 2011). Dermoscopy is currently used in melanoma surveillance to identify clinically significant nevi. Based on this study, the number of common acquired nevi with particular dermoscopic patterns may allow a slightly better assessment of melanoma risk. For each additional nonspecific nevus, the risk for melanoma increased by approximately 2%. The combined homogenous and/or complex nevus

types comprised 83% of our cohort; as such, this is consistent with the increased risk with increasing TNC. Incorporating globular and reticular numbers in the model increased the melanoma predictive accuracy by approximately 1%.

In this study, the rs12203592*T allele was strongly associated with the globular dermoscopic nevus pattern, with the homozygous *T/T genotype reducing globular nevus counts. This observation is consistent with the report in the SONIC study of children (with a mean age of 10.4 years) (Orlow et al., 2015) where the rs12203592*T allele was associated with a lower probability of having a globular morphology (than the homogenous pattern), even though it increased the total nevus count. As reported previously, adult *T/T carriers have reduced TNC, the reverse to that observed in children where *T/T have higher TNC (Duffy et al., 2010).

ETHICS STATEMENTS

This study was approved by the Metro South Human Research Ethics Committee (approval #HREC/09/QPAH/162, 26 August 2009) and The University of Queensland (approval #2009001590, 14 October 2009) and conducted in accordance with the Declaration of Helsinki. Participants provided written consent after receiving a Participant Information and Consent Form.

Data availability statement

Access to the dataset is available by arrangement with the corresponding author. Owing to the identifying nature of the dataset, it will not be placed in an open-access repository.

ORCIDs

David L. Duffy https://orcid.org/0000-0001-7227-632X
Kasturee Jagirdar https://orcid.org/0000-0001-8761-132X
Katie J. Lee https://orcid.org/0000-0002-9000-3226
Seamus R. McWhirter https://orcid.org/0000-0001-6682-3024
Erin K. McMeniman https://orcid.org/0000-0002-7834-1134
Annette Pflugfelder https://orcid.org/0000-0001-7858-0453
Jenna E. Rayner https://orcid.org/0000-0002-8288-0245
David C. Whiteman https://orcid.org/0000-0003-2563-9559
Matthew A. Brown https://orcid.org/0000-0003-0538-8211
N.G. Martin https://orcid.org/0000-0003-4069-8020
B.M. Smithers https://orcid.org/0000-0002-8333-8685
Helmut Schaider https://orcid.org/0000-0003-3195-2517
H. Peter Soyer https://orcid.org/0000-0002-4770-561X
Richard A. Sturm https://orcid.org/0000-0003-1301-0294

CONFLICT OF INTEREST

HPS is a shareholder of MoleMap NZ Limited and e-derm consult GmbH and undertakes regular teledermatological reporting for both companies. HPS is a Medical Consultant for Canfield Scientific Inc., a Medical Advisor for First Derm, and has a Medical Advisory Board Appointment with MoleMap NZ Limited. DLD, KJ, KJL, SRM, EKM, BD, AP, JER, DCW, MAB, NGM, SBS, HS, and RAS state no conflicts of interest.

ACKNOWLEDGMENTS

We thank all the BNMS volunteers for their participation. This work was funded by NHMRC project grant numbers 1004999, 1062935, and the Centre of Research Excellence for the Study of Nevi 1099021. The QSkin Study is supported by NHMRC program grant 1073898. The BLTS was supported most recently by NHMRC project 1031119 to NM. AP received a UQI tuition fee scholarship and a student living stipend. RAS was a Senior Research Fellow of the Australian NHMRC 1043187. HPS holds an NHMRC MRFF Next Generation Clinical Researchers Program Practitioner Fellowship 1137127. DCW is an NHMRC Principal Research Fellow 1058522, and MAB is an NHMRC Senior Principal Research Fellow 1024879. This research was carried out at the Translational Research Institute, Woolloongabba, Qld 4102, Australia. The Translational Research Institute is supported by a grant from the Australian Government.

Funding bodies had no role in the study design, collection, analysis, and interpretation of the data, writing the report, or publication decisions.

AUTHOR CONTRIBUTIONS

Conceptualization: HS, DLD, BMS, HPS, RAS; Data Curation:, DLD, KJ, KJL; Formal Analysis: DLD, KJ, RAS; Funding Acquisition: DLD, DCW, MAB, BMS, HS, HPS, RAS; Investigation: DLD, KJ, KJL, SRM, AP, JER; Methodology: DLD, DCW, HPS, RAS; Project Administration: HPS, RAS; Resources: EKM, BDA, DCW, MAB, NGM, BMS, HS, HPS, RAS; Software: DLD; Supervision: HPS, RAS; Validation: DLD, KJ, KJL, SRM, AP; Visualization: DLD; Writing - Original Draft Preparation: DLD, RAS; Writing - Review and Editing: DLD, KJ, KJL, SRM, EKM, BDA, AP, JER, DCW, MAB, NGM, BMS, HS, HPS, RAS

David L. Duffy[1,2], Kasturee Jagirdar[1], Katie J. Lee[1], Seamus R. McWhirter[1], Erin K. McMeniman[1,3], Brian De'Ambrosis[4], Annette Pflugfelder[1,5], Jenna E. Rayner[1], David C. Whiteman[2], Matthew A. Brown[6], N.G. Martin[2], B.M. Smithers[7], Helmut Schaider[1], H. Peter Soyer[1,3] and Richard A. Sturm[1,*]

[1]Dermatology Research Centre, The University of Queensland Diamantina Institute, The University of Queensland, Brisbane, Australia; [2]QIMR Berghofer Medical Research Institute, Brisbane, Australia; [3]Department of Dermatology, Princess Alexandra Hospital, Brisbane, Australia; [4]South East Dermatology, Annerley Square, Annerley, Brisbane, Australia; [5]Center of Dermatooncology, Department of Dermatology, University of Tübingen, Germany; [6]Translational Genomics Group, Institute of Health and Biomedical Innovation, Queensland University of Technology, Brisbane, Australia; and [7]Queensland Melanoma Project, Princess Alexandra Hospital, Mater Research Institute, The University of Queensland, Brisbane, Australia
[*]Corresponding author e-mail: r.sturm@uq.edu.au

SUPPLEMENTARY MATERIAL

Supplementary material is linked to the online version of the paper at www.jidonline.org, and at https://doi.org/10.1016/j.jid.2019.05.032.

REFERENCES

Bajaj S, Dusza SW, Marchetti MA, Wu X, Fonseca M, Kose K, et al. Growth-curve modeling of nevi with a peripheral globular pattern. JAMA Dermatol 2015;151:1338–45.

Bataille V, Bishop JA, Sasieni P, Swerdlow AJ, Pinney E, Griffiths K, et al. Risk of cutaneous melanoma in relation to the numbers, types and sites of naevi: a case-control study. Br J Cancer 1996;73:1605–11.

Blake T, McClenahan P, Duffy D, Schaider H, McEniery E, Soyer HP. Distribution analyses of acquired melanocytic naevi on the trunk. Dermatol Basel Switzerland 2014;228:269–75.

Duffy DL, Iles MM, Glass D, Zhu G, Barrett JH, Höiom V, et al. IRF4 variants have age-specific effects on nevus count and predispose to melanoma. Am J Hum Genet 2010;87:6–16.

Duffy DL, Zhu G, Li X, Sanna M, Iles MM, Jacobs LC, et al. Novel pleiotropic risk loci for melanoma and nevus density implicate multiple biological pathways. Nat Commun 2018;9:4774.

Fonseca M, Marchetti MA, Chung E, Dusza SW, Burnett ME, Marghoob AA, et al. Cross-sectional analysis of the dermoscopic patterns and structures of melanocytic naevi on the back and legs of adolescents. Br J Dermatol 2015;173:1486–93.

Law MH, Bishop DT, Lee JE, Brossard M, Martin NG, Moses EK, et al. Genome-wide meta-analysis identifies five new susceptibility loci for cutaneous malignant melanoma. Nat Genet 2015;47:987–95.

Lee S, Duffy DL, McClenahan P, Lee KJ, McEniery E, Burke B, et al. Heritability of naevus patterns in an adult twin cohort from the Brisbane Twin Registry: a cross-sectional study. Br J Dermatol 2016;174:356–63.

Marchetti MA, Kiuru MH, Busam KJ, Marghoob AA, Scope A, Dusza SW, et al. Melanocytic naevi with globular and reticular dermoscopic patterns display distinct BRAF V600E expression profiles and histopathological patterns. Br J Dermatol 2014;171:1060–5.

McWhirter SR, Duffy DL, Lee KJ, Wimberley G, McClenahan P, Ling N, et al. Classifying dermoscopic patterns of naevi in a case-control study of melanoma. PLOS ONE 2017;12:e0186647.

Orlow I, Satagopan JM, Berwick M, Enriquez HL, White KA, Cheung K, et al. Genetic factors associated with naevus count and dermoscopic patterns: preliminary results from the Study of Nevi in Children (SONIC). Br J Dermatol 2015;172:1081–9.

Ribero S, Zugna D, Osella-Abate S, Glass D, Nathan P, Spector T, et al. Prediction of high naevus count in a healthy UK population to estimate melanoma risk. Br J Dermatol 2016;174:312–8.

Suh KY, Bolognia JL. Signature nevi. J Am Acad Dermatol 2009;60:508–14.

Tan JM, Tom LN, Soyer HP, Stark MS. Defining the Molecular Genetics of dermoscopic naevus patterns. Dermatol Basel Switzerland 2019;235:19–34.

Zalaudek I, Schmid K, Marghoob AA, Scope A, Manzo M, Moscarella E, et al. Frequency of dermoscopic nevus subtypes by age and body site: a cross-sectional study. Arch Dermatol 2011;147:663–70.

SUPPLEMENTARY MATERIAL

Introduction

Epidemiological studies have shown that fair skin type, freckling, and high total body nevus counts (TNC) predispose to cutaneous melanoma (CM) (Berwick et al., 2016). The progression from melanocyte to nevus cell toward CM can occur through several independent pathways (Bennett, 2016; Damsky and Bosenberg, 2017; Shain and Bastian, 2016) that are each influenced by these host risk factors. The somatic genetic damage that drives CM development is strongly influenced by the density and type of skin melanin, pigmentation gene polymorphism, DNA damage response and propensity for nevus formation, and environmental sun exposure (Shain et al., 2018; Shain et al., 2015; Stark et al., 2018). Although the level, intensity and frequency of skin exposure to solar UV radiation are key environmental risk factors for CM, there is not a linear dose relationship, with acute and/or intermittent sun exposure being disproportionately effective. The most important single genetic determinant of sun sensitivity and CM risk in populations of European ancestry is variation within the *MC1R* locus, where multiple alleles are associated with the red hair color phenotype (RHC).

The morphological classification of the acquired melanocytic nevi observed through dermoscopy, including reticular, globular, and homogenous and/or complex (Argenziano et al., 2007), has recently been the subject of an in-depth review (Tan et al., 2019). These are the most common nevi that develop after birth, may be typical or atypical in appearance, and are considered benign. Histopathologically, these nevi are classed on the anatomical location within the skin, where they appear as discrete nests of melanocytic and/or nevus cells (Damsky and Bosenberg, 2017). The three major categories are junctional, where pigmented cells are confined to the epidermis; intradermal, where the cells are confined to the dermis; and compound, with both an epidermal and dermal component. Despite the histopathological differences, these acquired nevi have been thought to share a similar developmental pathway and relationship to melanoma, but independent pathways have been suggested to explain their formation (Zalaudek et al., 2007b). Two cytological features of nevus cells are clustering into nests and maturation. These features can provide a morphological basis to the patterns observed by dermoscopy (Marghoob, 2012). Maturation is a feature whereby there is a gradual change in cell shape and pigment content, with deeper lesions having a reduced nest size, cell, and nuclear content resulting in changes in cell shape (Damsky and Bosenberg, 2017). Longitudinal data have observed that reticular and globular nevi can change to the homogenous and/or structureless pattern with age (Zalaudek et al., 2011a; Zalaudek et al., 2011b) and are likely to represent a heterogenous group of nevi. Globular nevi are typically compound or dermal nevi with the globules corresponding to the nest of melanocytic cells at the dermal-epidermal junction, papillary dermis, or entirely in the dermis. Reticular nevi are usually junctional with the pigment network corresponding to a layer of pigmented nevus and keratinocytes along the basal layer of the regularly elongated rete ridges of the dermal-epidermal junction, or nests of melanocytic cells accumulated at the tips of these elongated rete ridges, appearing as pigmented lines and the suprapapillary plates as less-pigmented holes, conferring the network appearance.

It remains unclear how these different nevus types relate to other CM risk factors. It has been proposed that analysis of the nevus and dermoscopic diversity of each patient (intra-individual comparative analysis) would allow one to identify "the ugly duckling", that is, suspicious lesions worthy of further attention (Wazaefi et al., 2013). The diameter of a nevus also has prognostic significance, with malignant transformation more likely in those larger than 5 mm (Hofmann-Wellenhof et al., 2016), possibly mediated via increased telomere length (Bataille et al., 2007) or an inherent ability to overcome senescence (Bonet et al., 2017). Using candidate analysis of *MC1R* variant alleles and 85 other genes (Orlow et al., 2015), variants in several loci were associated with dermoscopic patterns observed during childhood, supporting the idea that genetic factors will strongly influence nevus morphology, as well as numbers in adults (Duffy et al., 2018).

Polymorphisms within four genes, *IRF4, MTAP, PLA2G6,* and *MITF*, have been shown to strongly influence TNC. A single polymorphism within an intronic region of the *IRF4* gene, rs12203592*C/T, shows a strong genotype-by-age interaction on the nevus count (Duffy et al., 2010) and is a major influence on pigmentation traits (Praetorius et al., 2013), tryosinase expression, and INFγ-induced gene regulation (Chhabra et al., 2018; Praetorius et al., 2013). The association between TNC and single nucleotide polymorphism (SNPs) upstream of the *MTAP* gene, adjacent to the well-known tumor suppressor gene *CDKN2A* on chromosome 9p21, and the *PLA2G6* gene on chromosome 22q13 exhibit less variable effects (Newton-Bishop et al., 2010). The fourth gene, *MITF*, has a coding region E318K allele that has also been shown to have a significant effect on nevus count, pigmentation, and melanomagenesis (Bassoli et al., 2018; Bonet et al., 2017; Sturm et al., 2014), but because the variant is uncommon, it has a lesser population level impact. Other nevus-associated genes have been recognized from a meta-analysis of 11 nevus genome-wide association study (GWAS) from Australia, Netherlands, United Kingdom, and the USA comprising over 50,000 phenotyped individuals (Duffy et al., 2018). This confirms that the strongest TNC-associated SNPs are within the *IRF4*, *MTAP*, and *PLA2G6* genes and has detected new loci at or near a genome-wide level of significance.

MATERIALS AND METHODS

Study samples

Melanoma patients observed between October 2009 and November 2016 were recruited from the Melanoma Unit and Dermatology Department of the Princess Alexandra Hospital , private practices drawing clients from Southeast Queensland or the Queensland Cancer Registry (Daley et al., 2017; Sturm et al., 2014) (Supplementary Table S6). Controls (no personal but possible first degree family history of CM) were obtained by the

advertisement of our study within the Princess Alexandra Hospital and by direct contact by letter of participants in the Brisbane Longitudinal Twin Study (Duffy et al., 2010) or QSkin participants (Olsen et al., 2012).

Measures and dermoscopy

All participants underwent detailed physical examination, including whole body digital images, nevus counts, and dermoscopic imaging performed by a trained research assistant on nevi ≥ 5mm in diameter. Photographs from 16 body sites and individual dermoscopic images of all significant nevi were recorded for 793 participants with a system for sequential total body photography and dermoscopy (FotoFinder Systems GmbH, Bad Birnbach, Germany) and a 3-dimensional total body image and dermoscopic images for 471 participants using a Vectra WB360 3-dimensional body imager (Canfield Scientific , Parsippany, NJ). As described in detail elsewhere (McWhirter et al., 2017), all the nevi ≥ 5mm were classified in terms of the predominant dermoscopic pattern using one of two methods (old and new BNMS [Brisbane Nevus Morphology Study] classification systems) that were integrated for analysis. Counting all nevi ≥ 2mm on the back in a subset of 572 individuals showed a high correlation with TNC ≥ 5mm (Supplementary Table S7). A clinical assessment using standardized pigmentation characteristics was performed as described (Ainger et al., 2017; Koh et al., 2018; Sturm et al., 2014).

Biospecimen collection

We report the analysis of 1,266 participants representing the BNMS (including 27 monozygotic and 39 dizygotic twins), 1,235 of whom provided saliva samples using an Oragene-DNA self-collection kit (DNA Genotec, Ottowa, Canada) sufficient for genomic DNA processing. Genomic DNA was extracted from 2 ml of saliva collected, and its quality and quantity was checked using Nanodrop UV absorbance and a Qubit fluorometer (Thermo Fisher, Waltham, MA). A minimum of 2.5 ug of DNA was then used for genotyping on the Infinium HumanCoreExome-24 Microarray (Illumina, San Diego, CA).

DNA sequencing and genotyping

Large scale SNP genotyping was performed using the Infinium Microarray HumanCoreExome-24 Chip (Illumina) as previously described (Daley et al., 2017), and the data was manipulated using the PLINK program (Chang et al., 2015). Genotype data were cleaned using a standard pipeline excluding SNPs exhibiting extreme Hardy-Weinberg disequilibrium and between-batch heterogeneity. Single SNP genotyping was performed using TaqMan SNP genotyping assays (Thermo Fisher Scientific, Waltham, MA) (Cook et al., 2009) in a 96 or 384 well plate format using a 7500 real-time PCR system and analyzed using 7500 Software (Applied Biosystems, Foster City, CA). The *MC1R* coding variants V60L, R163Q, and D294H, not included on the Illumina array, were genotyped by TaqMan assay C_7519054_10, C_7519060_20, and C_1010501_30 (ThermoFisher), respectively. Half the sample set were also subjected to automated DNA sequence analysis of PCR-amplified fragments covering the *MC1R* coding region (Box et al., 2001), and where identified *MITF* E318K variant rs149617956*G/A containing exon 9 (Yokoyama et al., 2011) using ABI PRISM Big Dye Terminator Sequencing (Applied Biosystems) with reactions processed by the Australian Equine Genetics Research Centre (AEGRC, Brisbane, Australia).

For the melanoma case-control analysis, we used an external set of general population controls (i.e., unknown melanoma status) to maximize the statistical power (this was not possible for dermoscopically classified nevus counts). Australian samples were from the QIMR Brisbane Longitudinal Twin Study (Daley et al., 2017) and QSkin samples (Olsen et al., 2019). In the case of the MITF rs149617956 SNP, instead we used the United Kingdom Biobank frequency (Bycroft et al., 2018), as this was not available on most of the external genotyping arrays. We excluded all SNPs exhibiting Hardy-Weinberg disequilibrium in controls with exact Hardy-Weinberg test $P < 0.0001$ and/or absent homozygotes despite the presence of heterozygotes, and those individuals with >3% genotyping failure. We retained related individuals, and the analyses have appropriately adjusted for this fact, such as a GEMMA mixed model analysis using the empirical kinship matrices and generalized linear mixed models or gene-dropping based on known pedigree relationships. The presented GWAS only used directly genotyped markers, but in addition, we have imputed key candidate SNPs from the regions reported to be associated with melanoma or total nevus count in Duffy et al (2018). The imputation of these regions was performed using BEAGLE5 (Browning et al., 2018).

Statistical analysis of datasets

Statistical analyses were carried out in the R Statistical Computing Environment (version 2.6.0, R Foundation for Statistical Computing, Vienna, Austria) and the GEMMA mixed model association computer package (Zhou and Stephens, 2012, 2014). Because we include related cases and controls in our analyses, linear and logistic regression analyses were carried out using the lme4 package in R (Bates et al., 2015). Based on the results from Box-Cox regression analyses, we chose to log transform the nevus counts ($\log_{10}$[count+1]). Since the nevus counts varied by age in a nonlinear fashion, we included linear and quadratic age terms as covariates, along with sex and the nevus counting protocol. For the genome-wide association analyses, we included melanoma case status as a covariate, since this variable has such a strong association with the nevus count, as well as the first four principal components. To perform the SNP genotype-based principal components analysis of ancestry, we used the TRACE computer package (Wang et al., 2015). This estimates principal components scores for our study participants with respect to an external reference panel (the Human Genome Diversity Panel). The default four principal component scores from this analysis were used as covariates in the association analyses. Alhough the mean age is different between the case and control, there are sufficient numbers in each age band to allow us to correctly model the relationship

between age and nevus count, as discussed elsewhere (Duffy et al., 2019). Aside from TNC, the variables that we study are constant over age, such as genotype. Q-Q plots for the GWAS analysis are presented in Supplementary Figure S3. A $P < 5x10^{-8}$ for each SNP was used as the cut off for genome-wide statistical significance, and $P < 5x10^{-7}$ suggestive of significance. For 33 candidate SNPs, the Bonferroni corrected critical threshold for one trait (experiment-wise $\alpha < 0.05$) would be 0.0015.

Data availability statement

Access to the dataset is available by arrangement with the corresponding author. Owing to the identifying nature of the dataset, it will not be placed in an open-access repository.

RESULTS

BNMS participants' demographics and phenotype

The study sample consisted of 1,266 individuals with counts of nevi of different dermoscopic morphology, the majority of European ancestry with minor contributions from Asia and Oceania (Supplementary Figure S4). There were 607 CM cases and 659 unaffected controls (Supplementary Table S1), with an enrichment of multiple primary melanoma cases; 275 participants (45% of the case participants) had two or more CM. The average age of the cases (55.5 years) was older than the controls (39.7 years), reflecting the oversampling (Supplementary Figure S5) of younger controls from the Brisbane Longitudinal Twin Study (Duffy et al., 2018) for whom we have longitudinal TNC (Lee et al., 2016). There were slightly more male cases (52.7%) but fewer male controls (44.6%). Skin (fair), hair (red), and eye (blue/gray) color were all associated with CM risk, with the frequency distribution of hair color in the control participants closely matching that from other Australian population studies (Supplementary Table S8). Melanoma cases had more than twice as many nevi $\geq$ 5mm diameter at any age (average case 31.4, control 13.3) and more freckles. The cases were heavier than the controls (average body mass index 28.1 vs 25.2), again reflecting the average age difference, but did not differ from the age-matched Queenslanders (Olsen et al., 2012).

Nevus subtypes called in this study and relationship to melanoma

The distribution plots of TNC in the cases and controls by age and dermoscopic nevus subtype are shown in Supplementary Figure S1. In each case for TNC, nonspecific, and reticular subtype regression curves for the cases are higher than those of the controls, with counts peaking at approximately age 50 years and then declining. The exception to this pattern was the globular subtype, in which the regression curves for both the cases and controls decline from 20 years of age, consistent with other reports (Zalaudek et al., 2006, 2011b).

GWAS of nevus subtypes in the BNMS and melanoma risk

The two SNPs on chromosome 1, rs4970612 and rs7545703, reached suggestive significance for TNC and reticular but not nonspecific nevus types, indicating a possible reticular-specific effect. However, these singleton SNPs were not associated with TNC in the large nevus meta-analysis (Duffy et al., 2018) and do not lie in regions of functional significance for melanocytes (Supplementary Table S9).

Effect of Nevogenic Genotype on TNC and Nevus Subtypes

We have plotted the nevus count distribution by the genotype of SNPs from the three genes most highly linked with TNC or a nevus subtype (Supplementary Table S5), (i) *MTAP* rs7023329*A/G, (ii) *PLA2G6* rs132985*C/T, and (iii) *IRF4* rs12203592*C/T (Supplementary Figures S6 and S7, Supplementary Table S10). The significant association with globular nevi for *IRF4* is seen by rs12203592*C/C as having greater number and rs12203592*T/T as the lowest median globular counts ($\beta = 9.55x10^{-2}$). *MTAP* rs7023329*A/A versus *G/G ($\beta = 5.24x10^{-2}$) and *PLA2G6* rs132985*C/C versus *T/T ($\beta = 4.32x10^{-2}$) show similar but smaller effects on the median globular counts. Consistent with this, the *MTAP* rs7023329*A/A and *PLA2G6* rs132985*C/C also had the greater number of TNC and reticular nevus counts. However, the rs12203592*T/T genotype was associated with the lowest globular nevi and the greatest number of nonspecific nevi.

Although the *MC1R* peak SNP associated with CM was not in itself linked to TNC or any dermoscopic nevus subtype (Supplementary Table S5), we have previously shown that when considered by *MC1R* variant allele classification as *MC1R*WT*, *MC1R*r*, and *MC1R*R* (Ainger et al., 2017), the *MC1R*R/r* genotype does act to modify TNC (Duffy et al., 2019). The *MC1R*R/r* and *MC1R*R/R* genotypes, which have the highest association with CM, were demonstrated to have a significant association with the nonspecific nevus subtype compared to the *MC1R*WT* genotype ($P = 1.4x10^{-8}$) using the model in Supplementary Table S11.

Interaction of nevus genes in TNC

The genetic interaction between *MTAP* and *PLA2G6* TNC-associated SNPs in the determination of nevus counts can be observed in Supplementary Figure S8, which plots the median TNC by combined genotype. There is a progressive decrease in the count from a maximum of 25 observed with *MTAP* rs7023329*A/A, *PLA2G6* rs132985*C/C risk genotype to a minimum of 8 observed with *MTAP* rs7023329*G/G, *PLA2G6* rs132985*T/T, with the stepwise progression the most obvious with the heterozygosity of *MTAP* rs7023329*A/G with the changing genotype at *PLA2G6* rs132985*C/C, *C/T, *T/T (green shading in Supplementary Figure S8).

DISCUSSION

The observation that host factors, including pigmentary skin type, are associated with the nevus count, density, distribution, and dermoscopic subtype (Zalaudek et al., 2007a, 2011a, 2011b) supports a role for genetic factors in the development and morphology of acquired melanocytic lesions. Given the effect sizes of known loci on TNC, we expected the statistical power of our study to be sufficient to detect the effects on subtype counts only in the candidate loci. Fortunately, we had results from our earlier large meta-analysis to guide us in selecting 33 chromosomal regions (including

MITF): 13 of 33 (39%) gave a *P*-value < 0.01 for melanoma, 5 of 33 (15%) for TNC, 5 of 33 (15%) for nonspecific nevi, 4 of 33 (12%) for globular nevi, and 2 of 33 (6%) for reticular nevi. The *MTAP* gene reached significance for all nevus properties assayed, the *PLA2G6* and *MITF* genes for three, and *IRF4* and *SLC45A2* for two. All the genes associated with the nevus phenotypes were also significantly associated with melanoma.

Multiple GWAS have implicated the SNP rs12203592*C/T within the fourth intron of the *IRF4* gene to be associated with skin pigmentation, hair and eye color, UVR sensitivity, CM susceptibility, tanning and facial pigmented spots (Han et al., 2008; Jacobs et al., 2015; Nan et al., 2009), nevus counts, and iris freckling (Duffy et al., 2010; Laino et al., 2018). In this study, we see that *T/T carriers have a lower TNC, especially in our CM cases (interaction $P = 0.005$, Supplementary Tables S12 and S13, Supplementary Figure S9). Recently, the rs12203592*T allele has been associated with CM, solar elastosis, and inversely with neval remnants (Gibbs et al., 2016), increased Breslow thickness of tumors (Gibbs et al., 2017), and decreased CM survival (Potrony et al., 2017). In melanocytic cells, we previously assigned a function for the IRF4 protein as a transcriptional regulator of the *TYR* gene (Chhabra et al., 2018; Praetorius et al., 2013), with the rs12203592*T allele reducing the IRF4 protein expression. There were also effects of rs12203592*T on melanocyte strain growth, response to UVR treatment, and IFNγ cytokine induction. It is highly likely that there is a melanocyte intrinsic effect of the rs12203592*T allele on globular nevus formation and involution. IRF4 is best known for its immunological roles, and IFNγ is likely to affect melanocyte behavior (Natarajan et al., 2014; Son et al., 2014). We demonstrated that elicited immune cell responses in the skin are modulated by the rs12203592 genotype (Chhabra et al., 2018), but the genotypic effects of *IRF4* on the melanocytic DNA repair (*cf MC1R*'s known role) are yet to be studied. Notably, the characterization of somatic genetic damage has shown significantly fewer copy number aberrations in globular compared to reticular nevi (Stark et al., 2018), implicating an *IRF4* polymorphism in this process.

The *MTAP* rs7023329 and *PLA2G6* rs11570734 SNPs were found to be the most informative for predicting TNC in the BNMS, with the *MTAP* gene polymorphism associated with all the dermoscopic nevus patterns. The function of these genes in the formation of nevi and CM is not known, but in the case of *MTAP*, these are linked to differential gene expression levels driven by elements linked to rs7023329 (Sangalli et al., 2017). *PLA2G6* encodes $iPLA_2\beta$-VIA, a protein that is essential for membrane remodeling in neurons and that has variable enzymatic activity depending on which phospholipids comprise these membranes. Morphologically characteristic axonal degeneration in a group of "*PLA2G6*-associated neurodegeneration" (PLAN) diseases is thought to be because of the degeneration of specific membranes (Sumi-Akamaru et al., 2015).

Our earlier findings supported the hypothesis that that individuals carrying the *MC1R* RHC genotypes tend to have fewer nevi (Duffy et al., 2004). In this study, we found that the RHC allele homozygotes (*MC1R*R/R*) had lower counts than the *MC1R*R* heterozygote carriers, but this latter group had higher counts than the wild type carriers on average (Supplementary Table S11). This seems consistent with a mixture of mechanisms acting on skin color lightening and longitudinal effects on nevus counts, as has been suggested in the case of *IRF4* genotype and CM risk (Duffy et al., 2010; Gibbs et al., 2017). In another study of nevus and freckle phenotypes in children (Barón et al., 2014), it was reported that sun exposure patterns can interact with *MC1R* RHC and *OCA2* variant genotypes to influence TNC, with the report that *MC1R*R/r*, *MC1R*R/R* together with homozygosity for *OCA2* rs12913832*C blue eye color alleles had elevated nevus counts. The rs4778138 SNP assayed here as the most informative SNP within the *OCA2* locus was significant at $P < 0.05$ for CM, TNC, and nonspecific nevi (Supplementary Table S5) in adults. However, the *MC1R*R/r*, *MC1R*R/R* genotypes were a greater influence, increasing nonspecific nevus counts in the BNMS (Supplementary Table S11). *MC1R* RHC variants have been shown to be associated with hypopigmentation, reduced structure of dermoscopic patterns, and more discernible vessels in benign, atypical, and CM lesions (Bassoli et al., 2013; Cuéllar et al., 2009; Quint et al., 2012). Another recent study of the influence of the *MC1R* genotype on the dermoscopic features of nevi found that R-allele carriers had visible vessels, dots, and globules present in their lesions, with eccentric hyperpigmentation (Vallone et al., 2018). Together, these studies and the BNMS (Duffy et al., 2019) indicate that *MC1R* RHC alleles are correlated with the nevus phenotype, including TNC, dermoscopic pattern, and body site distribution (Vallone et al., 2018).

Overall, the range of genes and biological pathways identified in this study of TNC and nevus morphology indicate that multiple biological pathways will be involved in nevogenesis (Duffy et al., 2018).

REFERENCES

Ainger SA, Jagirdar K, Lee KJ, Soyer HP, Sturm RA. Skin pigmentation genetics for the clinic. Dermatol Basel Switzerland 2017;233:1–15.

Argenziano G, Zalaudek I, Ferrara G, Hofmann-Wellenhof R, Soyer HP. Proposal of a new classification system for melanocytic naevi. Br J Dermatol 2007;157:217–27.

Barón AE, Asdigian NL, Gonzalez V, Aalborg J, Terzian T, Stiegmann RA, et al. Interactions between ultraviolet light and MC1R and OCA2 variants are determinants of childhood nevus and freckle phenotypes. Cancer Epidemiol Biomarkers Prev 2014;23:2829–39.

Bassoli S, Maurichi A, Rodolfo M, Casari A, Frigerio S, Pupelli G, et al. CDKN2A and MC1R variants influence dermoscopic and confocal features of benign melanocytic lesions in multiple melanoma patients. Exp Dermatol 2013;22:411–6.

Bassoli S, Pellegrini C, Longo C, Di Nardo L, Farnetani F, Cesinaro AM, et al. Clinical, dermoscopic, and confocal features of nevi and melanomas in a multiple primary melanoma patient with the MITF p.E318K homozygous mutation. Melanoma Res 2018;28:166–9.

Bataille V, Kato BS, Falchi M, Gardner J, Kimura M, Lens M, et al. Nevus size and number are associated with telomere length and represent potential markers of a decreased senescence in vivo. Cancer Epidemiol Biomarkers Prev 2007;16:1499–502.

Bates D, Mächler M, Bolker B, Walker S. Fitting linear mixed-effects models using lme4. J Stat Soft 2015;67:1–48.

Bennett DC. Genetics of melanoma progression: the rise and fall of cell senescence. Pigment Cell Melanoma Res 2016;29:122–40.

Berwick M, Buller DB, Cust A, Gallagher R, Lee TK, Meyskens F, et al. Melanoma Epidemiology and Prevention. Cancer Treat Res 2016;167:17–49.

Bonet C, Luciani F, Ottavi JF, Leclerc J, Jouenne FM, Boncompagni M, et al. Deciphering the Role of Oncogenic MITFE318K in Senescence Delay and Melanoma Progression. J Natl Cancer Inst 2017;109:djw340.

Box NF, Duffy DL, Chen W, Stark M, Martin NG, Sturm RA, et al. MC1R genotype modifies risk of melanoma in families segregating CDKN2A mutations. Am J Hum Genet 2001;69:765–73.

Browning BL, Zhou Y, Browning SR. A one-penny imputed genome from next-generation reference panels. Am J Hum Genet 2018;103:338–48.

Bycroft C, Freeman C, Petkova D, Band G, Elliott LT, Sharp K, et al. The UK Biobank resource with deep phenotyping and genomic data. Nature 2018;562:203–9.

Chang CC, Chow CC, Tellier LC, Vattikuti S, Purcell SM, Lee JJ. Second-generation PLINK: rising to the challenge of larger and richer datasets. GigaScience 2015;4:7.

Chhabra Y, Yong HXL, Fane ME, Soogrim A, Lim W, Mahiuddin DN, et al. Genetic variation in IRF4 expression modulates growth characteristics, tyrosinase expression and interferon-gamma response in melanocytic cells. Pigment Cell Melanoma Res 2018;31:51–63.

Cook AL, Chen W, Thurber AE, Smit DJ, Smith AG, Bladen TG, et al. Analysis of cultured human melanocytes based on polymorphisms within the SLC45A2/MATP, SLC24A5/NCKX5, and OCA2/P loci. J Invest Dermatol 2009;129:392–405.

Cuéllar F, Puig S, Kolm I, Puig-Butille J, Zaballos P, Martí-Laborda R, et al. Dermoscopic features of melanomas associated with MC1R variants in Spanish CDKN2A mutation carriers. Br J Dermatol 2009;160:48–53. https://doi.org/10.1111/j.1365-2133.2008.08826.x.

Daley GM, Duffy DL, Pflugfelder A, Jagirdar K, Lee KJ, Yong XLH, et al. GSTP1 does not modify MC1R effects on melanoma risk. Exp Dermatol 2017;26:730–3. https://doi.org/10.1111/exd.13114.

Damsky WE, Bosenberg M. Melanocytic nevi and melanoma: unraveling a complex relationship. Oncogene 2017;36:5771–92.

Duffy DL, Box NF, Chen W, Palmer JS, Montgomery GW, James MR, et al. Interactive effects of MC1R and OCA2 on melanoma risk phenotypes. Hum Mol Genet 2004;13:447–61.

Duffy DL, Iles MM, Glass D, Zhu G, Barrett JH, Höiom V, et al. IRF4 variants have age-specific effects on nevus count and predispose to melanoma. Am J Hum Genet 2010;87:6–16.

Duffy DL, Lee KJ, Jagirdar K, Pflugfelder A, Stark MS, McMeniman EK, et al. High naevus count and MC1R red hair alleles contribute synergistically to increased melanoma risk. Br J Dermatol 2019;181:1009–16.

Duffy DL, Zhu G, Li X, Sanna M, Iles MM, Jacobs LC, et al. Novel pleiotropic risk loci for melanoma and nevus density implicate multiple biological pathways. Nat Commun 2018;9:4774.

Gibbs DC, Orlow I, Bramson JI, Kanetsky PA, Luo L, Kricker A, et al. Association of interferon regulatory Factor-4 polymorphism rs12203592 with divergent melanoma pathways. J Natl Cancer Inst 2016;108.

Gibbs DC, Ward SV, Orlow I, Cadby G, Kanetsky PA, Luo L, et al. Functional melanoma-risk variant IRF4 rs12203592 associated with Breslow thickness: a pooled international study of primary melanomas. Br J Dermatol 2017;177:e180–2.

Han J, Kraft P, Nan H, Guo Q, Chen C, Qureshi A, et al. A genome-wide association study identifies novel alleles associated with hair color and skin pigmentation. PLOS Genet 2008;4:e1000074.

Hofmann-Wellenhof R, Marghoob AA, Zalaudek I. Large Acquired Nevus or Dysplastic Nevus: What's in the Name of a Nevus? JAMA Dermatol 2016;152:623–4.

Jacobs LC, Hamer MA, Gunn DA, Deelen J, Lall JS, van Heemst D, et al. A Genome-Wide Association study identifies the skin color genes IRF4, MC1R, ASIP, and BNC2 influencing facial pigmented spots. J Invest Dermatol 2015;135:1735–42.

Koh U, Janda M, Aitken JF, Duffy DL, Menzies S, Sturm RA, et al. Mind your Moles' study: protocol of a prospective cohort study of melanocytic nevi. BMJ, (Open) 2018;8:e025857.

Laino AM, Berry EG, Jagirdar K, Lee KJ, Duffy DL, Soyer HP, et al. Iris pigmented lesions as a marker of cutaneous melanoma risk: an Australian case-control study. Br J Dermatol 2018;178:1119–27.

Lee S, Duffy DL, McClenahan P, Lee KJ, McEniery E, Burke B, et al. Heritability of naevus patterns in an adult twin cohort from the Brisbane Twin Registry: a cross-sectional study. Br J Dermatol 2016;174:356–63.

Marghoob AA, editor. Nevogenesis: mechanisms and clinical implications of nevus development. Heidelberg: Springer; 2012.

McWhirter SR, Duffy DL, Lee KJ, Wimberley G, McClenahan P, Ling N, et al. Classifying dermoscopic patterns of naevi in a case-control study of melanoma. PLOS One 2017;12:e0186647.

Nan H, Kraft P, Qureshi AA, Guo Q, Chen C, Hankinson SE, et al. Genome-wide association study of tanning phenotype in a population of European ancestry. J Invest Dermatol 2009;129:2250–7.

Natarajan VT, Ganju P, Singh A, Vijayan V, Kirty K, Yadav S, et al. IFN-gamma signaling maintains skin pigmentation homeostasis through regulation of melanosome maturation. Proc Natl Acad Sci U S A 2014;111:2301–6.

Newton-Bishop JA, Chang YM, Iles MM, Taylor JC, Bakker B, Chan M, et al. Melanocytic nevi, nevus genes, and melanoma risk in a large case-control study in the United Kingdom. Cancer Epidemiol Biomarkers Prev 2010;19:2043–54.

Olsen CM, Green AC, Neale RE, Webb PM, Cicero RA, Jackman LM, et al. Cohort profile: the QSkin Sun and Health Study International. Int J Epidemiol 2012;41. 929-929i.

Olsen CM, Pandeya N, Thompson BS, Dusingize JC, Green AC, Neale RE, et al. Association between phenotypic Characteristics and Melanoma in a Large Prospective Cohort Study. J Invest Dermatol 2019;139:665–72.

Potrony M, Rebollo-Morell A, Giménez-Xavier P, Zimmer L, Puig-Butille JA, Tell-Marti G, et al. IRF4 rs12203592 functional variant and melanoma survival. Int J Cancer 2017;140:1845–9.

Praetorius C, Grill C, Stacey SN, Metcalf AM, Gorkin DU, Robinson KC, et al. A polymorphism in IRF4 affects human pigmentation through a tyrosinase-dependent MITF/TFAP2A pathway. Cell 2013;155:1022–33.

Quint KD, Van der Rhee JI, Gruis NA, Ter Huurne JA, Wolterbeek R, Van der Stoep N, et al. Melanocortin 1 receptor (MC1R) variants in high melanoma risk patients are associated with specific dermoscopic ABCD features. Acta Derm Venereol 2012;92:587–92.

Sangalli A, Malerba G, Tessari G, Rodolfo M, Gomez-Lira M. Melanoma risk alleles are associated with downregulation of the MTAP gene and hypermethylation of a CpG island upstream of the gene in dermal fibroblasts. Exp Dermatol 2017;26:733–6.

Shain AH, Yeh I, Kovalyshyn I, Sriharan A, Talevich E, Gagnon A, et al. The Genetic Evolution of Melanoma from Precursor Lesions. N Engl J Med 2015;373:1926–36.

Shain AH, Bastian BC. From melanocytes to melanomas. Nat Rev Cancer 2016;16:345–58.

Shain AH, Joseph NM, Yu R, Benhamida J, Liu S, Prow T, et al. Genomic and transcriptomic analysis reveals incremental disruption of key signaling pathways during melanoma evolution. Cancer Cell 2018;34:45–55.e4.

Son J, Kim M, Jou I, Park KC, Kang HY. IFN-gamma inhibits basal and alpha-MSH-induced melanogenesis. Pigment Cell Melanoma Res 2014;27:201–8.

Stark MS, Tan JM, Tom L, Jagirdar K, Lambie D, Schaider H, et al. Whole-exome sequencing of acquired nevi identifies mechanisms for development and maintenance of benign neoplasms. J Invest Dermatol 2018;138:1636–44. https://doi.org/10.1016/j.jid.2018.02.012.

Sturm RA, Fox C, McClenahan P, Jagirdar K, Ibarrola-Villava M, Banan P, et al. Phenotypic characterization of nevus and tumor patterns in MITF E318K mutation carrier melanoma patients. J Invest Dermatol 2014;134:141–9. https://doi.org/10.1038/jid.2013.272.

Sumi-Akamaru H, Beck G, Kato S, Mochizuki H. Neuroaxonal dystrophy in PLA2G6 knockout mice. Neuropathology 2015;35:289–302.

Tan JM, Tom LN, Soyer HP, Stark MS. Defining the Molecular Genetics of dermoscopic naevus patterns. Dermatol Basel Switzerland 2019;235:19–34.

Vallone MG, Tell-Marti G, Potrony M, Rebollo-Morell A, Badenas C, Puig-Butille JA, Gimenez-Xavier P, et al. Melanocortin 1 receptor (MC1R) polymorphisms' influence on size and dermoscopic features of nevi. Pigment Cell Melanoma Res 2018;31:39–50.

Wang C, Zhan X, Liang L, Abecasis GR, Lin X. Improved ancestry estimation for both genotyping and sequencing data using projection procrustes analysis and genotype imputation. Am J Hum Genet 2015;96:926–37.

Wazaefi Y, Gaudy-Marqueste C, Avril MF, Malvehy J, Pellacani G, Thomas L, et al. Evidence of a limited intra-individual diversity of nevi: intuitive perception of dominant clusters is a crucial step in the analysis of nevi by dermatologists. J Invest Dermatol 2013;133(10):2355–61.

Yokoyama S, Woods SL, Boyle GM, Aoude LG, MacGregor S, Zismann V, et al. A novel recurrent mutation in MITF predisposes to familial and sporadic melanoma. Nature 2011;480:99–103.

Zalaudek I, Argenziano G, Mordente I, Moscarella E, Corona R, Sera F, et al. Nevus type in dermoscopy is related to skin type in white persons. Arch Dermatol 2007a;143:351–6.

Zalaudek I, Catricalà C, Moscarella E, Argenziano G. What dermoscopy tells us about nevogenesis. J Dermatol 2011a;38:16–24.

Zalaudek I, Grinschgl S, Argenziano G, Marghoob AA, Blum A, Richtig E, et al. Age-related prevalence of dermoscopy patterns in acquired melanocytic naevi. Br J Dermatol 2006;154:299–304.

Zalaudek I, Hofmann-Wellenhof R, Kittler H, Argenziano G, Ferrara G, Petrillo L, et al. A dual concept of nevogenesis: theoretical considerations based on dermoscopic features of melanocytic nevi. J Dtsch Dermatol Ges. JDDG 2007b;5:985–92.

Zalaudek I, Schmid K, Marghoob AA, Scope A, Manzo M, Moscarella E, et al. Frequency of dermoscopic nevus subtypes by age and body site: a cross-sectional study. Arch Dermatol 2011b;147:663–70.

Zhou X, Stephens M. Genome-wide efficient mixed-model analysis for association studies. Nat Genet 2012;44:821–4.

Zhou X, Stephens M. Efficient multivariate linear mixed model algorithms for genome-wide association studies. Nat Methods 2014;11:407–9.

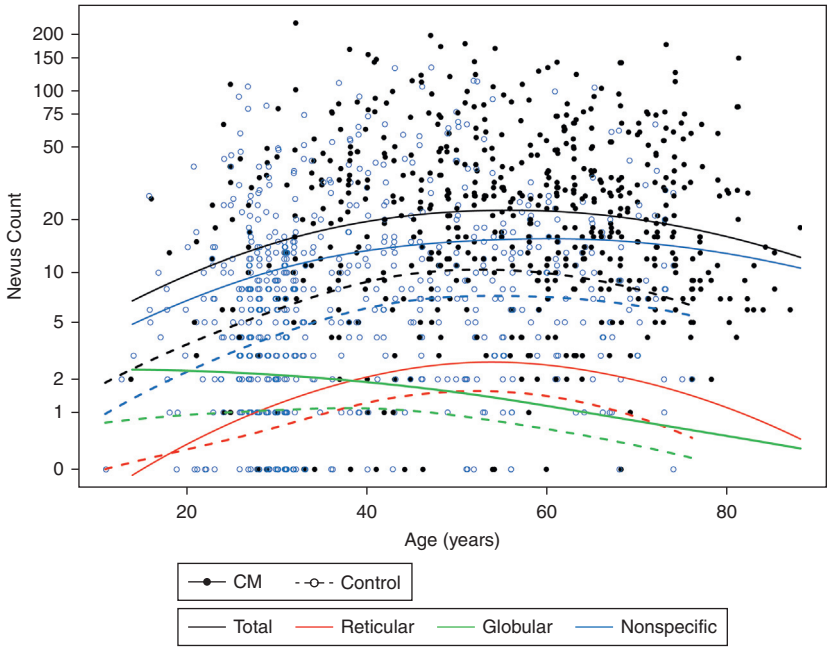

Supplementary Figure S1. Total nevus count by dermoscopic subtype and age. Scatter plot of TNC and dermoscopic nevus subtype body counts by age. Nevus count expressed on a logarithmic scale on the y-axis and age in years on the x-axis. Locally weighted regression curves for counts versus age in CM (full line) or control groups (dashed line), with colors representing nevus subtypes as indicated in the legend. CM, cutaneous melanoma.

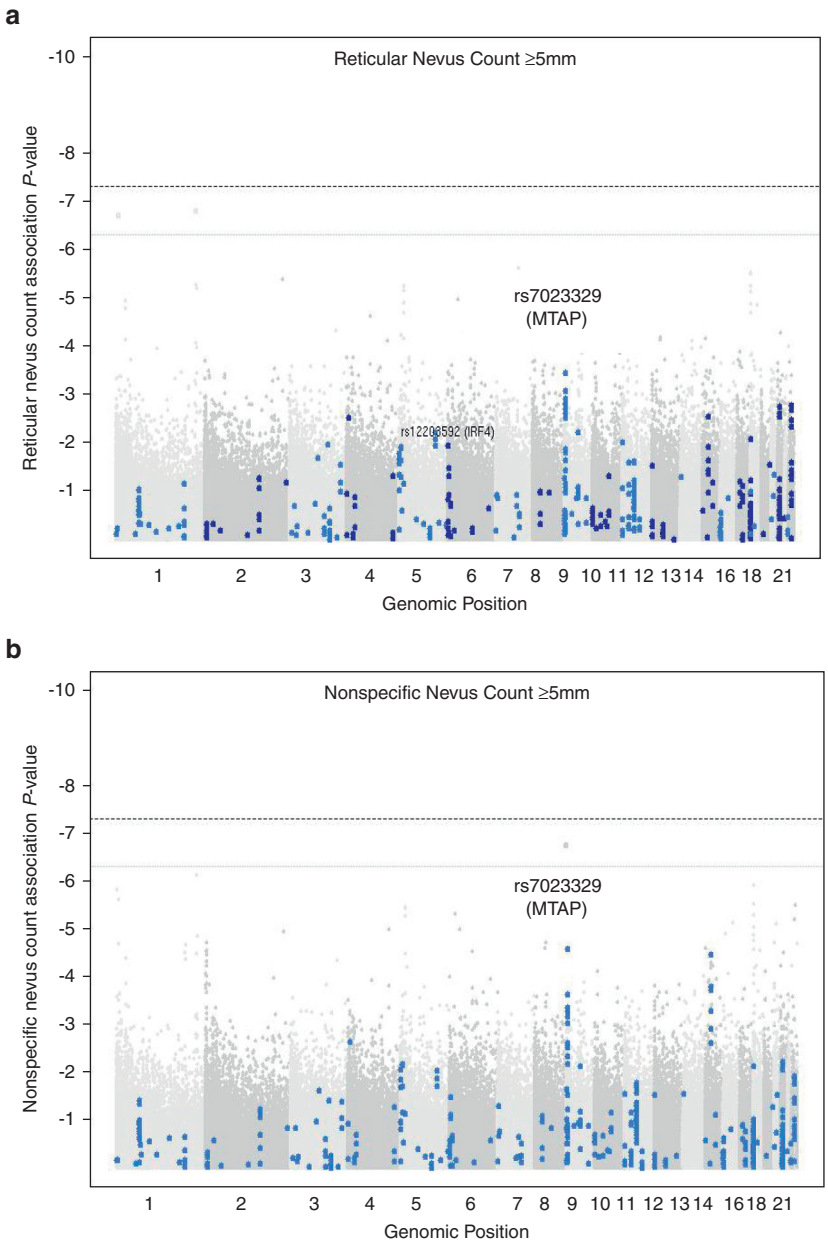

Supplementary Figure S2. GWAS plot for reticular and nonspecific nevus count. Manhattan plot of the *P*-values for (**a**) reticular and (**b**) nonspecific nevus count ≥ 5mm with genome-wide significance indicated by the black dashed line ($5x10^{-8}$) and suggestive of significance ($5x10^{-7}$) by the gray dotted line. Blue dots indicate the SNPs within previously association peaks, and the gray dots represent all the other SNPs on the Illumina HumanCoreExome array. The peak-associated SNP rs7023329 on chromosome 9 is indicated as *MTAP*. GWAS, genome-wide association study; SNP, single nucleotide polymorphism.

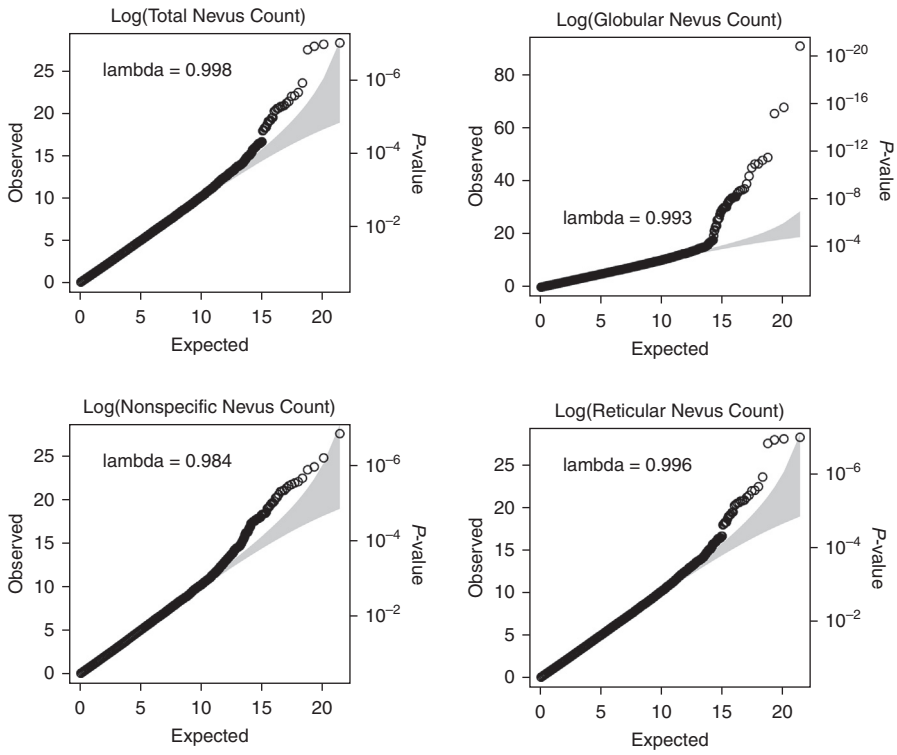

Supplementary Figure S3. Q-Q plots of GWAS for total and subtype nevus counts. The quantile-quantile (Q-Q) plots for genome-wide mixed model association analysis X-square of the four phenotypes: log-transformed TNC, nonspecific, globular, and reticular nevus counts. GWAS, genome-wide association study; TNC, total body nevus count.

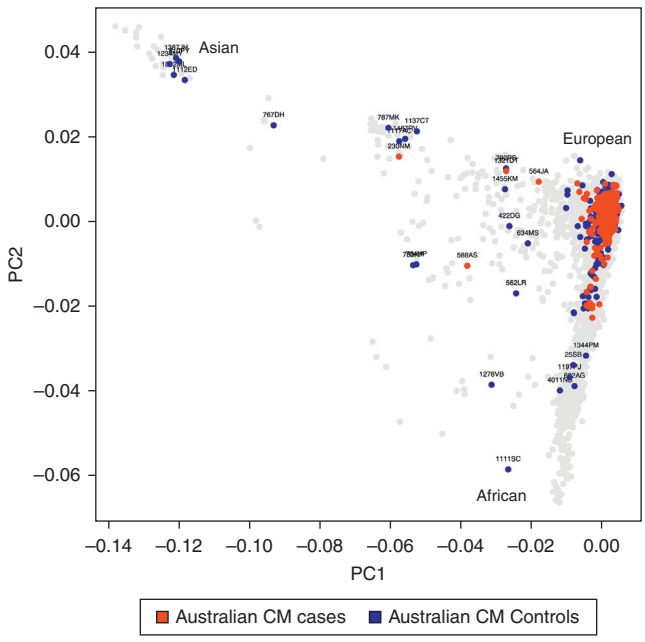

Supplementary Figure S4. Ancestry analysis by geneticprincipal components analysis. Plot of the first two components from the genetic principal components analysis of the BNMS participants CM cases (red) and unaffected (blue). These were supplemented by an additional 938 samples from the human genome diversity project in the TRACE computer package (gray) to maximize power to estimate the scores for BNMS participants. BNMS, Brisbane Nevus Morphology Study; CM, cutaneous melanoma; PC, principal component.

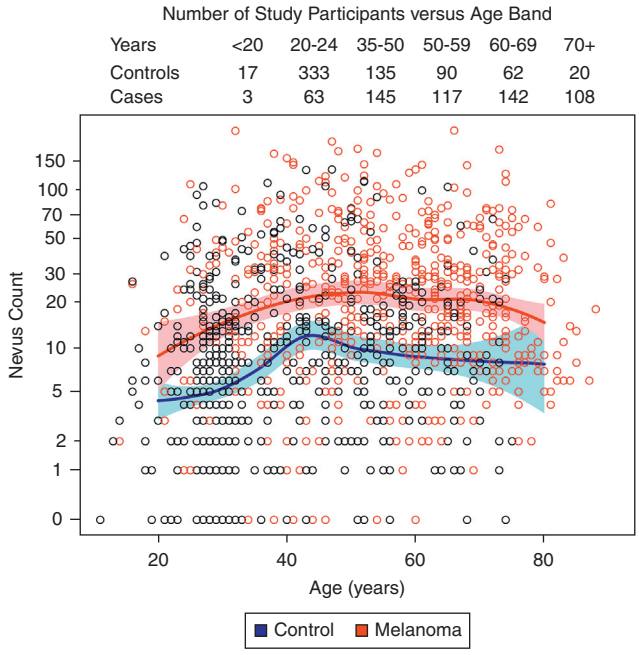

Supplementary Figure S5. Number of cases and controls at each age and its effect on the estimation of the relationship between age and nevus count ≥ 5mm. The upper panel provides counts of participation by age. The lower panel is a scatter plot of TNC ≥ 5mm by age and provides local confidence bands for age-nevus localized regression analysis fitted separately to cases and to controls using the R locfit package. The curves are roughly parallel over the entire age range, and shaded confidence bands of similar width except past the age of 70. For the critical phenotype of the nevus count, there is no evidence for bias or interaction that would affect the analysis combining cases and controls. TNC, total body nevus count.

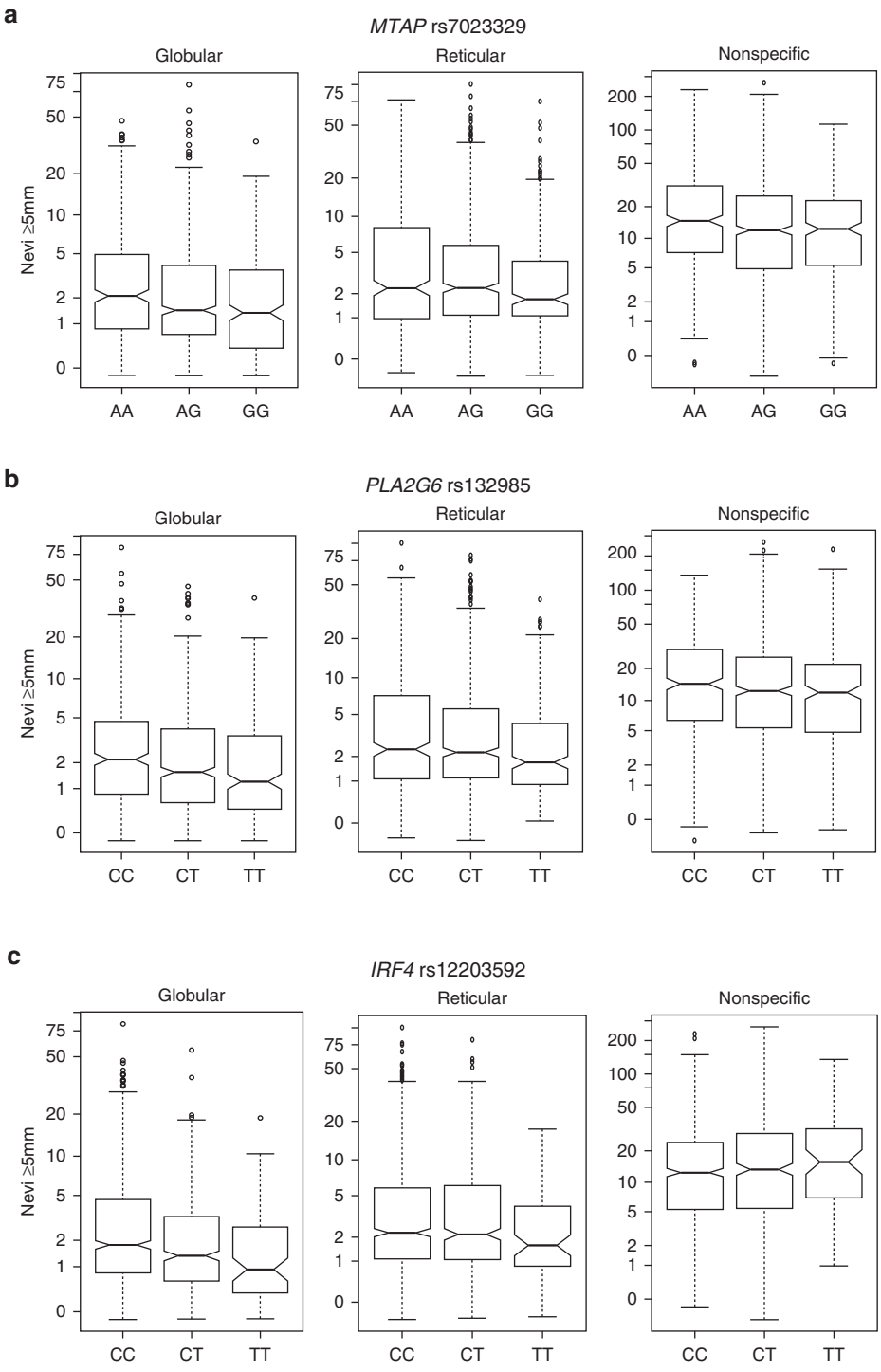

Supplementary Figure S6. *MTAP, PLA2G6,* and *IRF4* association with nevus dermoscopic subtypes. Three SNPs in genes previously linked with TNC were used to test for the association with the nevus count ≥ 5mm in the BNMS cohort. The box-and-whisker plots show the age, sex and classification method (McWhirter et al., 2017) adjusted median TNC on a logarithmic scale (solid bar; y-axis) presented by genotype (x-axis) for (**a**) *MTAP* rs7023329*A/G, (**b**) *PLA2G6* rs132985*C/T, (**c**) *IRF4* rs12203592*C/T in the samples subdivided into globular, reticular and nonspecific. The 75% to 25% limits are indicated by the upper and lower boxes and an approximate 95% confidence interval for the median by the vertical range of notches in the sides of the boxes around the median. The 97.5% upper and 2.5% lower range are the upper and lower extents of the vertical lines (whiskers) outside of the boxes with the outliers represented by empty circles. BNMS, Brisbane Nevus Morphology Study; SNP, single nucleotide polymorphism; TNC, total body nevus count.

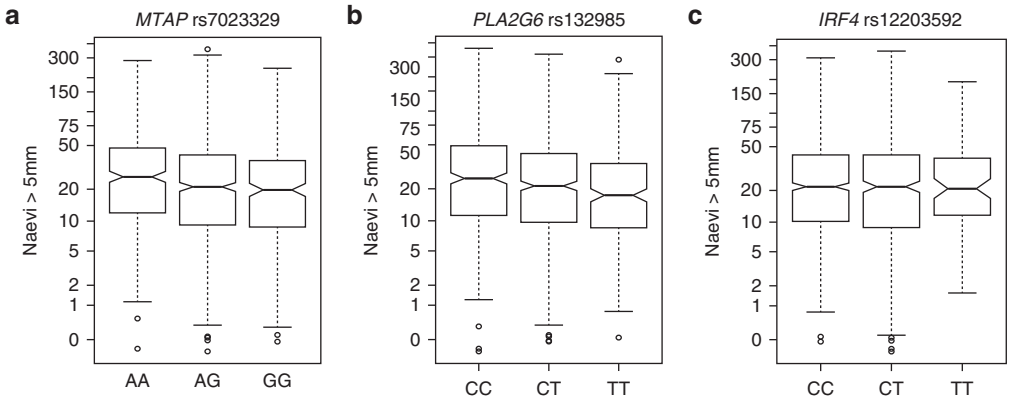

Supplementary Figure S7. *MTAP, PLA2G6,* and *IRF4* association with the total nevus count. The three SNPs from Figure 4 were used to test for association with TNC ≥ 5mm in the BNMS cohort. The box-and-whisker plots show the age, sex, and classification method (McWhirter et al., 2017) adjusted median TNC on a logarithmic scale (solid bar; y-axis) presented by genotype (x-axis) for (**a**) *MTAP* rs7023329*A/G, (**b**) *PLA2G6* rs132985*C/T, and (**c**) *IRF4* rs12203592*C/T. BNMS, Brisbane Nevus Morphology Study; SNP, single nucleotide polymorphism; TNC, total body nevus count.

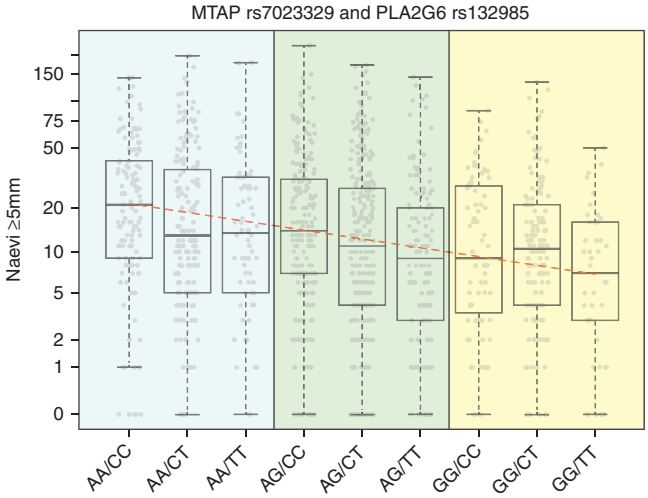

Supplementary Figure S8. *MTAP* and *PLA2G6* genotype have a synergistic effect on the nevus count. The combined genotypes at *MTAP* rs7023329*A/G and *PLA2G6* rs132985*C/T show a synergistic effect on the nevus count ≥5mm in the BNMS cohort. The box-and-whisker plots show the age, sex, and classification method (McWhirter et al., 2017) adjusted median TNC on a logarithmic scale (solid bar; y-axis) presented by genotype (x-axis). The *MTAP* rs7023329*A/A genotype is shaded blue, the rs7023329*A/T genotype shaded green, and the rs7023329*T/T genotype shaded yellow. BNMS, Brisbane Nevus Morphology Study; TNC, total body nevus count.

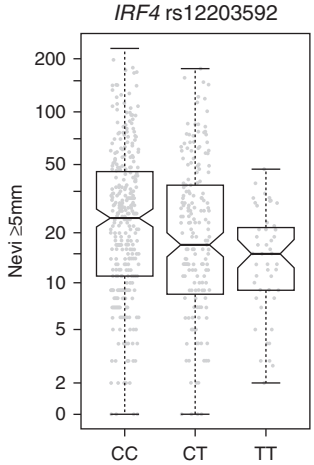

Supplementary Figure S9. *IRF4* association with the total nevus count in melanoma case participants. The association of *IRF4* rs12203592*C/T genotype with TNC is shown in the box-and-whiskers plot for cases only and unadjusted for any covariates. TNC, total body nevus count.

Supplementary Table S1. Demographic and Phenotypic Characteristics of 1,266 BNMS Participants

Characteristic	Total Mean (SD) or N (%)	Unaffected[1] Mean (SD) or N (%)	Case[2] Mean (SD) or N (%)	*P*-value[3]
Age (years)				$< 10^{-6}$
Male	49·9 ± 17·8	39·7 ± 15·0	59·2 ± 14·8	
Female	44·8 ± 15·6	39·6 ± 14·3	51·5 ± 14·6	
Total	47·3 ± 16·9	39·7 ± 14·6	55·5 ± 15·2	
Range	11-88	11-76	14-88	
Total N	1266	659	607	
Sex				0·007
Male	607 (48·4)	294 (44·6)	320 (52·7)	
Female	659 (51·6)	365 (55·7)	287 (47·3)	
Total N	1266	659	607	
Skin color				0·015
Fair	977 (77·7)	497 (75·5)	480 (80·1)	
Medium	242 (19·3)	133 (20·2)	109 (18·2)	
Olive	38 (3·0)	28 (4·3)	10 (1·7)	
Total N	1257	658	599	
Hair color				$1x10^{-5}$
Red	146 (11·5)	47 (7·2)	99 (16·4)	
Blonde	236 (18·8)	119 (18·1)	117 (19·4)	
Light brown	418 (33·0)	240 (36·6)	178 (29·5)	
Dark brown	400 (31·6)	219 (33·4)	181 (30·0)	
Black	59 (4·7)	31 (4·7)	28 (4·6)	
Total N	1259	656	603	
Eye color				$7x10^{-5}$
Blue/gray	676 (53·4)	329 (50·0)	347 (57·2)	
Green/hazel	371 (29·3)	187 (28·4)	184 (30·4)	
Brown	217 (17·1)	142 (21·6)	75 (12.4)	
Total N	1264	658	606	
Total Nevi Count ≥5mm mean +/- SD				$< 10^{-6}$
Globular	2.3 +/- 5.2	1.8 +/- 4.1	2.7 +/- 6.2	
Reticular	3.6 +/- 8.7	2.2 +/- 5.7	5.2 +/- 10.9	
Non-specific	16.4 +/- 22.4	9.3 +/- 13.6	24.2 +/- 27.1	
Total	22.0 +/- 28.5	13.3 +/- 18.9	31.4 +/- 33.7	
Total N	1266	659	607	
Combined Freckling Score[4]				$< 10^{-6}$
0 to 3	726 (59·1)	432 (66·1)	294 (51·1)	
3 to 6	406 (33·0)	178 (27·2)	228 (39·7)	
7 to 9	97 (7·9)	44 (6·7)	53 (9·2)	
Total N	1229	654	575	
Height (cm)				0·02
Male	178·0 ± 7·1	179·6 ± 6·9	176·6 ± 6·8	
Female	165·7 ± 6·9	166·3 ± 6·9	164·7 ± 6·4	
Total	171·6 ± 9·2	172·2 ± 9·5	171·0 ± 8·9	
Total N	1123	601	522	
Weight (kg)				$< 10^{-6}$
Male	85·4 ± 15·6	83·8 ± 14·7	87·4 ± 15·8	
Female	71·7 ± 17·1	67·8 ± 13·6	76·8 ± 19·4	
Total	78·4 ± 17·6	74·9 ± 16·2	82·4 ± 18·4	
Total N	1122	601	521	
Body mass index (kg/m^2)				$< 10^{-6}$
Male	26·9 ± 4·5	25·9 ± 4·0	28·0 ± 4·7	
Female	26·2 ± 6·2	24·5 ± 5·0	28·3 ± 7·0	
Total	26·5 ± 5·5	25·2 ± 4·6	28·1 ± 5·9	
Total N	1122	601	521	

Abbreviations: BNMS, Brisbane Nevus Morphology Study; SD, Standard deviation.
[1]Unaffected, participant with no prior history of melanoma
[2]Case, participant with prior history of at least one melanoma
[3]Unadjusted for other covariates
[4]Face, Shoulder, Hands (none = 0, mild = 1, moderate = 2, severe =3; 0 to 9 total)

Supplementary Table S2. Melanoma OR for Nevus Subtype Count Quintiles

Bar[1]	Level	Nevus Subtype[2]	Odds Ratio[3]	95% CI
1	Q2	Globular	1.01	0.60–1.71
2	Q2	Reticular	1.28	0.78–2.11
3	Q2	Nonspecific	1.78	1.14–2.81
4	Q3	Globular	1.52	0.91–2.58
5	Q3	Reticular	1.78	1.10–2.89
6	Q3	Nonspecific	2.37	1.52–3.74
7	Q4	Globular	1.46	0.87–2.49
8	Q4	Reticular	2.74	1.69–4.46
9	Q4	Nonspecific	4.27	2.73–6.76
10	Q5	Globular	2.82	1.72–4.88
11	Q5	Reticular	2.94	1.84–4.77
12	Q5	Nonspecific	7.64	4.86–12.19

Abbreviation: CI, confidence interval.

[1]Corresponding bar in Figure 1

[2]The first quintile for nonspecific nevus count (adjusted to that of a male aged 40 years) was 2.35, for reticular 0.20, and globular 0.34. These correspond to observed counts of 3, 1, and 0 (recalling that the regression adjustment for age can lead to a fractional count).

[3]Odds ratios for melanoma are relative to the lowest quintile.

Supplementary Table S3. Logistic Regression Analysis of CM Risk within a Subset of Individuals[1] with Separate Counts of Complex and Homogenous Pattern Nevi

Term	OR	95%LL	95%UL	*P*-value
(Intercept)	0.27	0.16	0.43	
Poly (Age, 2) linear	2.22×10^{14}	1.50×10^{9}	4.762×10^{19}	$< 2.2 \times 10^{-16}$
Poly (Age, 2) quadratic	2.77×10^{8}	3.50×10^{3}	2.49×10^{13}	4.0×10^{-15}
Sex (M)	0.84	0.58	1.21	0.76
[2]Complex Q2 (1,3)	1.52	0.89	2.62	9.1×10^{-9}
Q3 (3,6)	1.90	1.11	3.26	
Q4 (6,14)	2.46	1.42	4.30	
Q5 (14,112)	4.75	2.40	9.62	
[2]Homogenous Q2 (1,4)	2.04	1.18	3.54	2.2×10^{-16}
Q3 (4,8)	2.81	1.62	4.93	
Q4 (8,17)	3.74	2.08	6.81	
Q5 (17,101)	11.34	5.63	23.75	
[3]logReticular	1.09	0.87	1.36	0.17
[3]logGlobular	0.73	0.53	1.00	0.36

Abbreviations : CM, cutaneous melanoma; LL, lower limit; M, male; OR, odds ratio; UL, upper limit.

[1]359 cases and 323 controls

[2]These counts have been divided into quintiles

[3]log reticular and globular counts have been treated as continuous predictors

Supplementary Table S4. Logistic Regression Analysis of CM Risk within the BNMS Collection versus Age and Nevus Subtype Counts

Term	Beta	SE	Statistic	OR	95%LL	95%UL	*P*-value
(Intercept)	-1.70	0.2	-8.39	0.18	0.12	0.27	0.00
Age linear	12.66	2.58	4.91	313606	2012	48874478	0.00
Age quadratic	8.46	2.59	3.27	4728.25	29.51	757516.22	0.00
[1,2]Homogeneous	0.47	0.07	6.57	1.59	1.39	1.83	0.00
[1,2]Complex	0.31	0.07	4.30	1.36	1.18	1.56	0.00
[1]Globular	-0.19	0.11	-1.75	0.83	0.67	1.02	0.08
[1]Reticular	0.04	0.08	0.56	1.04	0.90	1.36	1.21

Abbreviations: BNMS, Brisbane Nevus Morphology Study; CM, cutaneous melanoma; LL, lower limit; OR, odds ratio; SE, standard error; UL, upper limit.
[1]Counts are $\log_2$ transformed, so the ORs represent the increase in risk for each doubling of that nevus count.
[2]Missing homogenous and complex counts have been imputed using the R mice package (5 replicates) using age, melanoma status, reticular, globular and total nevus counts.

Supplementary Table S5. [1]SNP Association with Melanoma, TNC and Nevus Subtypes in 1,235 BNMS Samples

SNP[2]	Chr:Position B37	Gene/Interval	Melanoma[4]	TNC	Nonspecific	Globular	Reticular
rs869329[c]	9: 21804693	*MTAP*	$5x10^{-9}$	$2x10^{-6}$	$7x10^{-5}$	$1x10^{-4}$	$2.7x10^{-3}$
rs132985	22: 38563471	*PLA2G6*	$1x10^{-4}$	$1.7x10^{-3}$	0.0139	$6.5x10^{-3}$	0.0296
rs12203592	6: 396321	*IRF4*	$4x10^{-8}$	0.0227	0.4499	$7x10^{-8}$	0.0909
rs10816595[c]	9: 110709735	9q31.2	$3.7x10^{-3}$	0.0846	0.0894	0.5221	0.4129
rs600951	9: 224742	*DOCK8*	0.0335	0.3742	0.1157	0.1319	0.2128
rs7313352	12: 88949124	*KITLG*	0.3831	0.7310	0.8718	0.1360	0.1747
rs4670813	2: 38317710	*CYP1B1*	0.0821	0.4003	0.7688	0.9480	0.2213
rs251464	5: 149196234	*PPARGC1B*	0.3249	0.0965	0.1855	0.3383	0.9078
rs55875066[3]	2: 240076002	*HDAC4*	0.1314	0.1256	0.2882	0.9024	0.0215
rs1640875	12: 13069524	*GPRC5A*	0.0143	0.6933	0.6703	0.4285	0.2666
rs45575338	10: 5784151	*FAM208B*	0.3631	0.6571	0.4502	0.6948	0.8358
rs12696304	3: 169481271	*TERC*	0.7276	0.4896	0.5087	0.2992	0.9124
rs117648907	15: 33277710	*FMN1*	$4x10^{-11}$	0.1412	0.1654	$2.1x10^{-3}$	0.1302
rs34466956	19: 3353622	*NFIC*	0.8102	0.8649	0.5558	0.4655	0.0150
rs2357176[3]	14: 64409313	*SYNE2*	0.7236	0.0265	$1.0x10^{-3}$	0.2516	0.3668
rs1484375[3]	9: 109067561	9q31.1	$3.1x10^{-3}$	0.0834	0.0693	0.9217	0.1288
rs2695237	1: 226603635	*PARP1*	0.7906	0.3463	0.7699	0.2807	0.1421
rs73008229	11: 108187689	*ATM*	0.0819	0.2336	0.3245	0.6375	0.7646
rs72704658	1: 150833010	*SETDB1*	0.7074	0.2450	0.1646	0.6592	0.9683
rs12596638	16: 54115829	*FTO*	0.0629	0.4483	0.4887	0.6338	0.6469
rs1636744	7: 16984280	*AGR3*	$1.2x10^{-3}$	0.2534	0.1918	0.6076	0.9715
rs416981	21: 42745414	*MX2*	$3.7x10^{-3}$	0.7200	0.7965	0.2918	0.1144
rs75570604	16: 89846677	*MC1R*	$6x10^{-7}$	0.2863	0.0400	0.5417	0.1148
rs380286	5: 1320247	*TERT*	$3.6x10^{-3}$	$7.6x10^{-3}$	$4.8x10^{-3}$	0.9069	0.3737
rs498136	11: 69367118	*TPCN2/CCND1*	0.6300	0.0469	0.0683	0.9377	0.0323
rs7582362	2: 202176294	*CASP8*	0.0277	0.2863	0.2486	0.7472	0.4071
rs56238684	20: 33236696	*ASIP*	$2x10^{-9}$	0.1501	0.0227	0.7066	0.1221
rs2125570	6: 21166705	*CDKAL1*	0.5263	0.1171	0.1123	0.7639	0.3278
rs10830253	11: 89028043	*TYR*	0.2307	0.2332	0.2135	0.7257	0.3319
rs184628474	14: 91185865	*TTC7B*	0.4401	0.3137	0.1233	0.7305	0.4347
rs250417[3]	5: 33952378	*SLC45A2*	$6x10^{-7}$	$2x10^{-5}$	$4x10^{-6}$	0.0357	0.1483
rs4778138	15: 28335820	*OCA2*	0.0125	0.0132	0.0205	0.3633	0.4730
rs149617956	3: 70014091	*MITF*	$2x10^{-18}$ [5]	$5x10^{-4}$	$2.0 x10^{-3}$	0.04	$5.0x10^{-3}$

Abbreviations: BNMS, Brisbane Nevus Morphology Study; SNP, single nucleotide polymorphism; TNC, total body nevus count.
[1]The SNP identified in a bivariate analysis of nevi and melanoma by Duffy et al., (2018), presented in the same order with inclusion of *MITF* E318K. Given that there are 33 candidate SNPs, the Bonferroni corrected critical threshold for one trait (experiment-wise $\alpha < 0.05$) would be 0.0015.
[2]The SNP was directly genotyped unless superscript 3.
[3]The SNP was imputed.
[4]Compared with 27,251 individuals directly genotyped in the QIMR Brisbane Longitudinal Twin Study and other studies combined with BNMS controls.
[5]Compared with 452,264 United Kingdom Biobank controls.

Supplementary Table S6. Source of BNMS Study Participants

Source	Cases N (%)	Unaffected controls N (%)	Total N (%)
Brisbane Longitudinal Twin Study	3 (0.49)	244 (37.03)	247 (19.51)
QSkin Study	2 (0.33)	73 (11.08)	75 (5.92)
Melanoma Patients Australia	22 (3.62)	13 (1.97)	35 (2.76)
Queensland Cancer Registry	5 (0.82)	0	5 (0.39)
Princess Alexandra Hospital Melanoma Surgical Unit, Dermatology Outpatients Department, Oncology Department	303 (49.92)	79 (11.99)	382 (30.17)
Private dermatology or primary care clinics	199 (32.78)	29 (4.4)	228 (18.01)
Volunteers - media coverage, advertising or word of mouth	58 (9.56)	154 (23.37)	212 (16.75)
Volunteers - family members of earlier participants	8 (1.32)	36 (5.46)	44 (3.48)
Other sources	7 (1.15)	31 (4.70)	48 (3.79)
Total (100%)	607	659	1266

Supplementary Table S7. Pearson Correlations for Log-Transformed Counts of TNC ≥ 5mm Diameter of Different Dermoscopic Appearance over Body, all Nevi 2-5 mm Diameter on the Back, and of Pigmented Lesions (Freckles and Nevi) of the Iris in Melanoma Cases and Controls: Nevi 2-5 mm Diameter were only Counted on 572 Individuals (213 Cases, 334 Controls) (Laino et al., 2018)

Log number	TNC ≥ 5mm	Non-specific ≥ 5mm	Globular ≥ 5mm	Reticular ≥ 5mm	Back nevi 2-5 mm	Iris pigmented lesions
TNC ≥ 5mm	1					
Non-specific ≥ 5mm	0.94	1				
Globular ≥ 5mm	0.50	0.33	1			
Reticular ≥ 5mm	0.50	0.30	0.45	1		
Back nevi 2-5 mm	0.61	0.50	0.50	0.70	1	
Iris pigmented lesions	0.22	0.21	0.02	0.09	0.17	1

Abbreviation: TNC, total body nevus count.

Supplementary Table S8. Hair and Eye Color in BNMS Controls, Compared to Large Australian Population-Based Studies

	Females			Males		
	[1]BNMS Control N (%)	[2]QSkin N (%)	[3]BMES N (%)	[1]BNMS Control N (%)	[2]QSkin N (%)	[3]BMES N (%)
Hair Color						
Black	14 (3.9)	1394 (5.9)	155 (7.7)	17 (5.8)	2971 (15.0)	169 (10.9)
Dark Brown	105 (28.9)	8195 (34.6)	1251 (61.8)	112 (38.5)	6313 (31.8)	973 (62.8)
Light Brown	145 (39.9)	8910 (37.6)		95 (32.6)	7186 (36.2)	
Blonde/Fair	75 (20.7)	3723 (15.7)	454 (22.4)	44 (15.1)	2366 (11.9)	319 (20.6)
Red	24 (6.6)	1482 (6.3)	165 (8.1)	23 (7.9)	993 (5.0)	88 (5.7)
Total (100%)	363	23,704	2025	291	19,829	1549
Eye Color						
Blue/Gray	184 (50.7)	8227 (35.2)	856 (45.6)	144 (56.8)	8110 (41.4)	821 (56.1)
Green/Hazel	102 (28.1)	9479 (40.6)	579 (30.8)	85 (26.5)	6613 (33.8)	362 (24.8)
Brown/Black	77 (21.2)	5669 (24,3)	445 (23.6)	64 (16.7)	4835 (24.7)	280 (19.1)
Total	363	23,375	1880	293	19,558	1463

Abbreviations: BMES, Blue Mountains Eye Study; BNMS, Brisbane Naevus Morphology Study.
[1]self-reported hair, observer eye color.
[2]QSkin: QSkin Sun and Health Study, self-reported hair and eye color.
[3]observer hair and eye color.

Supplementary Table S9. Association of Chromosomal Regions and SNPs with TNC and Nevus Subtype Counts in BNMS[1]

Phenotype	chr	rs number	position	Allele 1	Allele 0	Freq Allele 1	Beta	Standard error	*P*-value	Loci within region
Reticular	1	rs4970612	39125390	C	T	0.218	-0.119	0.0227	2.06e-07	RP11=334L9.1 RRAGC MYCBP RHBDL2
TNC	1	rs4970612	39125390	C	T	0.218	-0.119	0.0227	2.06e-07	RP11=334L9.1
TNC	1	rs7545703	240167654	C	T	0.629	0.103	0.0196	1.67e-07	RRAGC MYCBP RHBDL2 RPS7P5
Non-specific	1	rs7545703	240167654	C	T	0.629	0.097	0.0195	8.03e-07	RPS7P5
Reticular	1	rs7545703	240167654	C	T	0.629	0.104	0.0196	1.67e-07	
Globular	2	indel.59162	9547629	D	I	0.026	0.289	0.0414	8.51e-12	

Abbreviations: BNMS, Brisbane Nevus Morphology Study; SNP, single nucleotide polymorphism; TNC, total body nevus count.
[1]Association *P*-value, highest for TNC and includes the highest nevus subtype SNP where relevant.

Supplementary Table S10. *MTAP, PLA2G6,* and *IRF4* SNP Associations with TNC and Nevus Subtypes in 1,235 BNMS Samples Calculated Using the GEMMA Package

	Total Body			Globular			Reticular			Nonspecific		
Gene/SNP	Beta	SE	p-value	Beta	SE	p-value	Beta	SE	p-value	Beta	SE	p-value
MTAP rs7023329*A	8.07×10^{-2}	1.90×10^{-2}	2.3×10^{-5}	5.24×10^{-2}	1.48×10^{-2}	4.1×10^{-4}	8.06×10^{-2}	1.90×10^{-2}	2.31×10^{-5}	6.95×10^{-2}	1.89×10^{-2}	2.3×10^{-4}
PLA2G6 rs132985*C	5.89×10^{-2}	1.88×10^{-2}	1.7×10^{-3}	4.32×10^{-2}	1.46×10^{-2}	3.13×10^{-3}	5.89×10^{-2}	1.88×10^{-2}	1.7×10^{-3}	4.64×10^{-2}	1.87×10^{-2}	1.3×10^{-2}
IRF4 rs12203592*C	5.69×10^{-2}	2.26×10^{-2}	1.1×10^{-2}	9.55×10^{-2}	1.74×10^{-2}	6.04×10^{-8}	5.69×10^{-2}	2.25×10^{-2}	1.1×10^{-2}	1.82×10^{-2}	2.25×10^{-2}	4.1×10^{-1}

Abbreviations: BNMS, Brisbane Nevus Morphology Study; SNP, single nucleotide polymorphism; TNC, total body nevus count.

Supplementary Table S11. *MC1R* Variant Genotype Association with Melanoma, TNC and Nevus Subtypes in 1,235 BNMS Samples

MC1R Genotype	CM[1] OR (95% CI)	TNC[2] (95% CI)	Nonspecific (95% CI)	Globular (95% CI)	Reticular (95% CI)
WT/WT	1.00	8.9 [7.3–10.7]	5.6 [4.6–6.9]	0.6 [0.4–0.8]	2.0 [1.5–2.5]
WT/r	2.1 [1.4–3.2]	10.0 [8.3–12]	6.9 [5.6–8.3]	0.7 [0.5– 0.9]	1.9 [1.5–2.4]
r/r	3.0 [1.7–5.2]	10.2 [7.9–13.2]	7.5 [5.7–9.7]	0.4 [0.2–0.7]	2.0 [1.4 –2.7]
WT/R	2.9 [1.9–4.4]	10.5 [8.7–12.7]	7.7 [6.3–9.4]	0.6 [0.4–0.8]	1.7 [1.3– 2.2]
R/r	4.0 [2.6–6.2]	14.2 [11.7–17.3]	11.3 [9.2–13.8]	0.6 [0.4–0.8]	1.8 [1.4 –2.3]
R/R	5.6 [3.2–9.9]	9.9 [7.5–12.8]	8.9 [6.8–11.6]	0.4 [0.1–0.6]	1.0 [0.6–1.5]
P-value[3]	9.0×10^{-12}	3.9×10^{-4}	1.4×10^{-8}	0.17	0.015

Abbreviations: BNMS, Brisbane Nevus Morphology Study; CI, confidence interval; CM, cutaneous melanoma; OR, odds ratio; SNP, single nucleotide polymorphism; TNC, total body nevus count.

[1]Odds ratios for CM are from a logistic regression model adjusting for age, age squared, sex and four ancestry principal components.

[2]Nevus counts are predicted counts for that *MC1R* genotype for a 60 year aged male control of study average ancestry.

[3]Association *P*-value from linear model of log-transformed nevus count adjusting for age, age squared, sex and CM status, and four ancestry principal components.

Supplementary Table S12. *IRF4* Variant Genotype Interaction with Melanoma Status, TNC, and Nevus Subtypes[1]

CM status	rs12203592	TNC[2,3] (95% CI)	Nonspecific (95% CI)	Globular (95% CI)	Reticular (95% CI)
Case	C/C	25.3 [21.7–29.6]	16.1 [13.5–19]	1.6 [1.3–1.9]	3.7 [3–4.5]
	C/T	19.5 [16.2–23.4]	13.7 [11.2–6.7]	0.8 [0.6–1.1]	3.0 [2.3–3.8]
	T/T	15.8 [11.4 – 21.8]	18.7 [13.3–26.1]	0.5 [0.2–1]	2.2 [1.3–3.4]
Control	C/C	10.3 [8.4–12.5]	7.2 [5.9–8.8]	0.7 [0.5–1]	1.6 [1.3–2]
	C/T	11.3 [9–14.1]	8.4 [6.7–10.5]	0.6 [0.4–0.9]	1.8 [1.4–2.3]
	T/T	9.6 [6.2–14.6]	8.2 [5.3–12.4]	0.3 [0–0.7]	1.4 [0.8–2.3]

Abbreviations: CI, confidence interval; CM, cutaneous melanoma; TNC, total body nevus count.

[1]Tabulated counts are those predicted for a 60-year-old man with study-average values for the four ancestry principal components from a linear model for log-transformed nevus counts, including age, age squared, sex, and Principal components fitted separately to melanoma cases and controls.

[2]Difference between genotypic means for cases, P-value = 0.003

[3]Interaction P-value = 0.005. The full regression model for total body nevus count ≥ 5mm diameter including an interaction term for melanoma case and *IRF4* genotype finds that the difference between cases and controls is statistically significant, so the rs12203592*T allele decreases total body nevus count in cases only.

Supplementary Table S13. Model Results for *IRF4* Variant Genotype Interaction with Melanoma Status, TNC, and Nevus Subtypes

Model Term	Estimate	Std. Error	F value	P value
(Intercept)	0.2796147	0.1638953		
Poly (Age, 2) linear	1.5256929	0.8535486	82.5622	< 2.2e-16***
Poly (Age, 2) quadratic	-4.3619215	0.7495693		
Male Sex	0.0685030	0.0261406	11.2336	0.0008278***
Ancestry PC1	-0.0011170	0.0013784	16.6890	4.690e-05***
Ancestry PC2	0.0032572	0.0009198	17.9981	2.378e-05***
Ancestry PC3	0.0026545	0.0023422	2.1625	0.1416695
Ancestry PC4	-0.0029405	0.0017499	3.5328	0.0604037
Melanoma case	0.3898524	0.0350442	131.5341	< 2.2e-16***
rs12203592*T	0.0135493	0.0300765	5.1415	0.0235343*
Case:rs12203592*T	-0.1180755	0.0417879	7.9839	0.0047961**

Abbreviations: PC, principal component; Std, standard; TNC, total body nevus count. *P < 0.05; **P < 0.01; ***P < 0.001.

The full regression model for total body nevus count ≥ 5mm diameter. including an interaction term for melanoma case and *IRF4* genotype finds that the difference between cases and controls is statistically significant, so the rs12203592*T allele decreases the total body nevus count in cases only.